Cell PRESS
Structure
Short Article

Structure of the PolIIIα-τ_c-DNA Complex Suggests an Atomic Model of the Replisome

Bin Liu,[1,3] Jinzhong Lin,[1] and Thomas A. Steitz[1,2,3,*]
[1]Department of Molecular Biophysics and Biochemistry
[2]Department of Chemistry
Yale University, New Haven, CT 06520, USA
[3]Howard Hughes Medical Institute, New Haven, CT 06520, USA
*Correspondence: thomas.steitz@yale.edu
http://dx.doi.org/10.1016/j.str.2013.02.002

SUMMARY

The C-terminal domain (CTD) of the τ subunit of the clamp loader (τ_c) binds to both the DnaB helicase and the DNA polymerase III α subunit (PolIIIα), and determines their relative positions and orientations on the leading and lagging strands. Here, we present a 3.2 Å resolution structure of *Thermus aquaticus* PolIIIα in complex with τ_c and a DNA substrate. The structure reveals that the CTD of τ_c interacts with the CTD of PolIIIα through its C-terminal helix and the adjacent loop. Additionally, in this complex PolIIIα displays an open conformation that includes the reorientations of the oligonucleotide-binding fold and the thumb domain, which may be an indirect result of crystal packing due to the presence of the τ_c. Nevertheless, the position of the τ_c on PolIIIα allows us to suggest an approximate model for how the PolIIIα is oriented and positioned on the DnaB helicase.

INTRODUCTION

The replisome is a multiprotein machine that replicates chromosomal DNA. The essential components of the replisome are conserved and include the replicative hexameric helicase that encircles the lagging DNA strand and unwinds the duplex DNA, the primase that synthesizes short RNA primers (10–12 nt), and the DNA polymerase III holoenzyme (Yao and O'Donnell, 2009, 2010). In eubacteria, the replicative DNA PolIII core, the β-sliding clamp, and the clamp-loader complex assemble to form PolIII holoenzyme, the main replicase that is responsible for DNA synthesis (Johnson and O'Donnell, 2005; McHenry, 1988). The PolIII holoenzyme in *Escherichia coli* contains two PolIII cores composed of the catalytic α subunit (Maki and Kornberg, 1985), the 3′-5′ proofreading exonuclease ε subunit (Scheuermann and Echols, 1984), and the θ subunit, which is believed to stabilize the ε subunit and slightly stimulate its proofreading capabilities (Johnson and O'Donnell, 2005; Taft-Benz and Schaaper, 2004). The β-sliding clamp, which is assembled onto the RNA-primed initiation sites by the clamp-loader complex, is a homodimer that forms a ring surrounding the DNA substrates and ensures the high processivity of the PolIII holoenzyme (Georgescu et al., 2008a; Kong et al., 1992). The clamp-loader complex is a multisubunit ATPase ($\tau_3\delta\delta'\chi\psi$; Georgescu et al., 2012; Pritchard et al., 2000) that links the PolIII to the helicase via its τ subunits (Studwell-Vaughan and O'Donnell, 1991). The C-terminal domain (CTD) of *E. coli* τ (*Eco*τ) binds to both the PolIII core and DnaB helicase, holding them together (Gao and McHenry, 2001a, 2001b; Kim et al., 1996).

The interaction of PolIIIα with τ has been well studied in the *E. coli* system. Nuclear magnetic resonance (NMR) and surface plasmon resonance (SPR) experiments have shown that the last 18 residues of τ are critical for the interaction with PolIIIα (Jergic et al., 2007; Su et al., 2007). Mutagenesis studies on *Eco*PolIIIα have revealed that deletion and mutations of the C-terminal region of the polymerase severely diminish its interaction with τ, indicating a role of CTD in the interaction (Dohrmann and McHenry, 2005). Recent structural studies on PolIIIα (*Thermus aquaticus* PolIIIα [*Taq*PolIIIα], *E. coli* PolIIIα [*Eco*PolIIIα], and *Geobacillus kaustophilus* PolC [*Gka*PolC]) have provided structural insights into the mechanism of DNA replication and this interaction (Bailey et al., 2006; Evans et al., 2008; Lamers et al., 2006). PolIIIα contains six domains with different functions: the N-terminal Zn^{2+}-dependent 3′-5′ coproofreading exonuclease polymerase and histidinol phosphatase (PHP) domain (Stano et al., 2006; Wing et al., 2008), the catalytic palm domain, the incoming nucleotide-interacting fingers domain (Brautigam and Steitz, 1998), the nascent DNA gripping-thumb domain (Steitz, 1999), the β-sliding clamp-binding domain, and the CTD, which contains an oligonucleotide-binding (OB) fold and a possible external clamp-binding site at the extreme C terminus (López de Saro et al., 2003). The solution structure of domain V of *Eco*τ, which lies at its C terminus, contains six α helices interspersed with the strands of a three-β-sheet fold. However, the structure of the most C-terminal portion of PolIIIα that was believed to interact with τ is absent in the apo enzyme structure. Also, the sequence of the *E. coli* τ_c is not homologous to that of a few species, such as *T. aquaticus* and *T. thermophilus*. In order to provide structural insights into the replisome architecture in *T. aquaticus*, we determined the structure of *Taq*PolIIIα in complex with τ_c and a DNA substrate in the presence of deoxynucleotide triphosphates at 3.2 Å resolution through molecular replacement (MR) combined with single anomalous dispersion (SAD) using heavy atom derivatives. The structure shows that the CTD of τ_c interacts with the CTD of PolIIIα through its C-terminal helix and the adjacent loop, which provides a basis

Table 1. Data Collection and Refinement Statistics

Data Set	Native	Pt Derivative	Hg Derivative
Data Collection			
Wavelength (Å)	0.9999	1.0715	1.0093
Resolution (Å)[a]	50–3.20 (3.37–3.20)	50–3.80 (3.94–3.80)	50–3.60 (3.73–3.60)
Space group	$P2_1$	$P2_1$	$P2_1$
Cell dimension			
a, b, c (Å)	188.53, 94.97, 204.08	190.14, 94.86, 204.86	187.45, 95.81, 204.17
α, β, γ (°)	90.00, 89.97, 90.00	90.00, 90.01, 90.00	90.00, 90.12, 90.00
Completeness (%)[a]	93.8 (93.8)	99.9 (100)	99.8 (99.4)
Unique reflections[a]	112,427 (14,848)	71,832 (7,161)	84,784 (8,354)
Total reflections	265,336	478,720	620,862
$\langle I/\sigma I\rangle$ [a]	11.8 (1.8)	19.9 (1.1)	21.2 (2.1)
R_{sym} (%)[a,b]	4.4 (53.9)	9.2 (100)	13.5 (100)
Redundancy[a]	2.4 (2.3)	6.7 (6.4)	7.3 (7.1)
Copies in AU	4	4	4
Twin fraction[c]	0.30	0.43	0.29
Refinement			
Resolution (Å)	20–3.20		
Number of reflections	108,754		
R_{factor}/R_{free} (%)	26.63/30.47		
Rmsd			
Rmsd bond (Å)	0.010		
Rmsd angle (°)	1.272		
Ramachandran plot (%)			
Preferred regions	97.9		
Allowed regions	2.1		
Access code	4IQJ		

[a]Numbers in parentheses correspond to the highest-resolution shell.
[b]$R_{sym} = \Sigma|I - \langle I\rangle|/\Sigma I$, where I is the observed intensity and $\langle I\rangle$ is the averaged intensity of multiple observations of symmetry-related reflections.
[c]Twin fractions were estimated by the H test for twinning in SCALA.

for constructing an atomic model of the replisome structure. Interestingly, the structure of PolIIIα in this complex displays an open conformation that includes the movements in the CTD and thumb domains, which is distinct from the previous apo structure (Bailey et al., 2006) and the one with only DNA bound (Wing et al., 2008). This open conformation could be an indirect effect of τ_c on crystal packing.

RESULTS AND DISCUSSION

Overall Structure

There are four copies of the complex of *Taq*PolIIIα with τ_c and DNA per asymmetric unit, with each PolIIIα bound to one τ_c and one DNA (Table 1). In each copy, six domains of *Taq*PolIIIα (PHP, palm, fingers, thumb, β-binding, and CTD) are clearly organized as an irregular pyramid around the central active-site cavity with an open gate composed of the OB fold of CTD and the thumb domain (Figure 1; Figures S1–S3 available online).

The relative orientations of the domains in the four copies are not identical to each other. The structures of the PHP, palm, finger, and β-binding domains of the four copies in the asymmetric unit are similar (Figure S4), suggesting that these structural units are conformationally rigid. However, the relative positions and structures of the CTD, thumb domain, τ_c, and DNA substrates in the complex show some variations among the four copies, indicating their structural flexibilities (Figure S4). Moreover, the relative positions between the OB fold and the remaining portion of the CTD exhibited slight differences as well among the different copies.

The larger number of interactions among different subunits and copies resulted in more regions of PolIIIα being visible in the electron density map than in the map of the apo structure (Bailey et al., 2006). These include the extreme C terminus of PolIIIα (residues 1,206–1,220), which now clearly shows a helical conformation close to the C-terminal portion of τ_c; additional portions of the CTD (residues 1,081–1,093 and 1,055–1,066); and the whole loop (residues 282–305) linking the PHP and palm domains. The third metal atom in the cluster site of the PHP domain, which was predicted to be zinc but was replaced by a water molecule in the apo structure, was built with a zinc ion (Figure S5). Interestingly, the orientations of the three zinc ions and their coordinating residues are quite similar to those of cocatalytic zinc motifs containing nucleases, especially nuclease P1 (Romier et al., 1998).

The DNA substrate is positioned in a distinct state as compared with its orientation and location in the complex with only DNA bound (Wing et al., 2008). None of the DNA substrates in the four copies are positioned in the active-site cavity, and each one exhibits a slightly different binding orientation (Figure S4). They are located far from the catalytic site on the palm domain and are not bent. The incorporation of 2′,3′-dideoxycytidine-5′-triphosphate (ddCTP) into the DNA from one copy indicates that DNA synthesis should have happened in solution. The duplex portions are approximately parallel to the long axis of the β-binding domain and all are visible in the electron density. However, they end at the gate formed by the OB fold and the thumb domain and do not enter the active-site cavity (Figure 1). The 5′ single-stranded DNA (ssDNA) overhang portions, which lie in the cavity, could not be completely built and differ substantially among the four copies. The DNA substrates interact with PolIIIα with a contact area of ~500 Å^2 per copy, which is less than that of their intermolecular interactions (~610 Å^2 per copy). All of these observations, therefore, suggest that the orientation of these DNA substrates is mainly a result of their intermolecular crystal packing interactions.

τ_c Structure and the PolIIIα-τ_c Interaction

Sequence alignments show that *Taq*τ_c and *Tth*τ_c share a 54.3% sequence identity and 61.3% homology; however, *Taq*τ_c and *Eco*τ_c (composed mainly of domains IV and V) share only a 13.4% sequence identity and 20.3% homology, which means that *Taq*τ_c is homologous to *Tth*τ_c but not to *Eco*τ_c (Figure S6). This information is consistent with the structural differences between *Taq*τ_c and *Eco*τ_c observed here. The NMR structure of *Eco*τ domain V contains six α helices intermixed with a three-stranded β sheet (Su et al., 2007). However, the structure of *Taq*τ_c does not exhibit a similar fold; rather, it has two domains

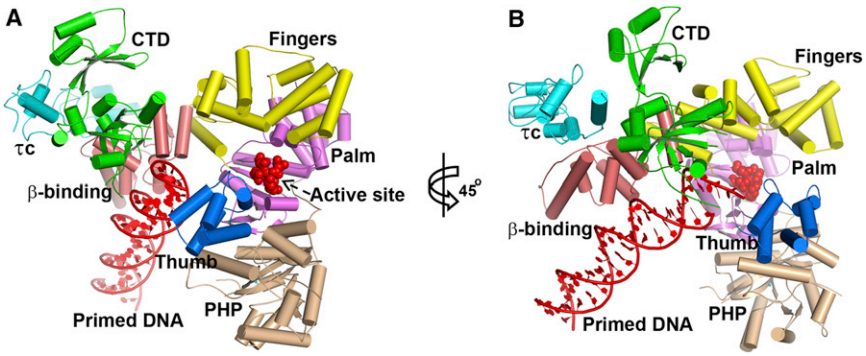

Figure 1. Cartoon Views of the PolIIIα-τc-DNA Complex

The primed DNA, τc structure, and the PHP, palm, thumb, finger, β-binding, and CTD domains of PolIIIα are labeled with red, cyan, wheat, violet, marine, yellow, salmon, and green colors, respectively. The active-site metal-binding residues (D463, D465, and D618) in the palm domain are shown with red spheres.

(A and B) The right panel in (B) is achieved by rotating the left one in (A) by 45° along the y axis of the figure plane.

See also Figures S1–S3.

that have only α helices and are linked by a proline-rich loop (Figure 2A). The linker loop (residues 460–486) is disordered and thus invisible in the map. The N-terminal domain (NTD) of *Taq*τc corresponds to *Eco*τ domain IV, which binds to both DnaB helicase and DNA (Jergic et al., 2007; Johnson and O'Donnell, 2005). In this structure, the NTD (involving residues 371–376) makes contact with the β-binding domain of PolIIIα, which may be a consequence of crystal packing interactions. However, the structure may also reveal a weak transient functional interaction. Interestingly, there is a cleft on the NTD that exhibits positive surface electrostatic potential (Figure 2B) and may be the region that has been proposed to bind DNA (Jergic et al., 2007). It is possible that we did not observe interactions between the ssDNA and τc here, because the length of the 5′ overhang was too short for the DNA to bind the N-terminal portion of τc and/or the binding orientation of the DNA seen here was not the catalytically relevant one.

The CTD of *Taq*τc interacts with the CTD of PolIIIα through its C-terminal helix (residues 531–543) and the following loop (residues 525–530; Figures 2C and 2D), which is consistent with previous work predicting that the C-terminal portion of *Eco*τc forms a helix-loop-helix structure to interact with PolIIIα (Jergic et al., 2007), and that the last 18 residues of *Eco*τc are critical for the PolIIIα-τc interaction (Su et al., 2007). These interactions do not appear to support the previous proposal that τ sequesters the polymerase tail from the β-sliding clamp (López de Saro et al., 2003). In *T. aquaticus*, the CTD of PolIIIα comprises an OB fold (residues 1,012–1,119), a putative τ-binding portion (residues 1,128–1,220), and an α-helix linker between them. The regions of PolIIIα that were observed binding to τc include the previously proposed portion, the linker helix, and the OB fold. The contact area between the CTD of τc and PolIIIα constitutes 52% of all the τc-PolIIIα interface areas (~650 Å^2).

The specific side-chain interactions made by the C-terminal helix of τc with the τ-binding portion of PolIIIα vary among the four copies, which may be due to the flexibility of the τ-binding portion (the average root-mean-square deviation [rmsd] of Cα atoms is 2.17 Å) and/or perturbation by the crystallization; however, the contacts between the loop of τc that follows the C-terminal helix and the CTD of PolIIIα show slight changes involving hydrophobic interactions and hydrogen bonds. Previous studies revealed that no single mutation in the region

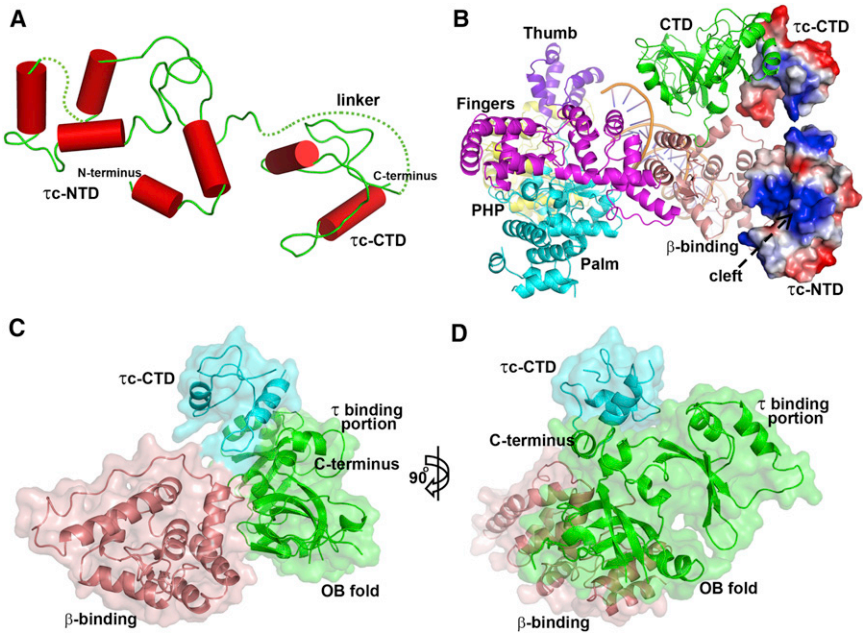

Figure 2. τc Structure and Interactions of the CTD of τc and the CTD of PolIIIα

(A) The structure of τc is composed of two domains that contain only α helices and are linked by a proline-rich linker. The dotted lines represent the disordered regions.

(B) The primed DNA and the six domains of PolIIIα are shown in a schematic representation with different colors, and τc is shown in an electrostatic surface representation using PyMOL. The positively charged cleft that may bind ssDNA on the NTD of τc is labeled.

(C and D) Surface representation shows the interaction regions of τc CTD and PolIIIα and their relative positions. The NTD of τc is omitted here. The right panel (D) is obtained by rotating the left one (C) by 90° along the y axis of the figure plane.

See also Figure S4.

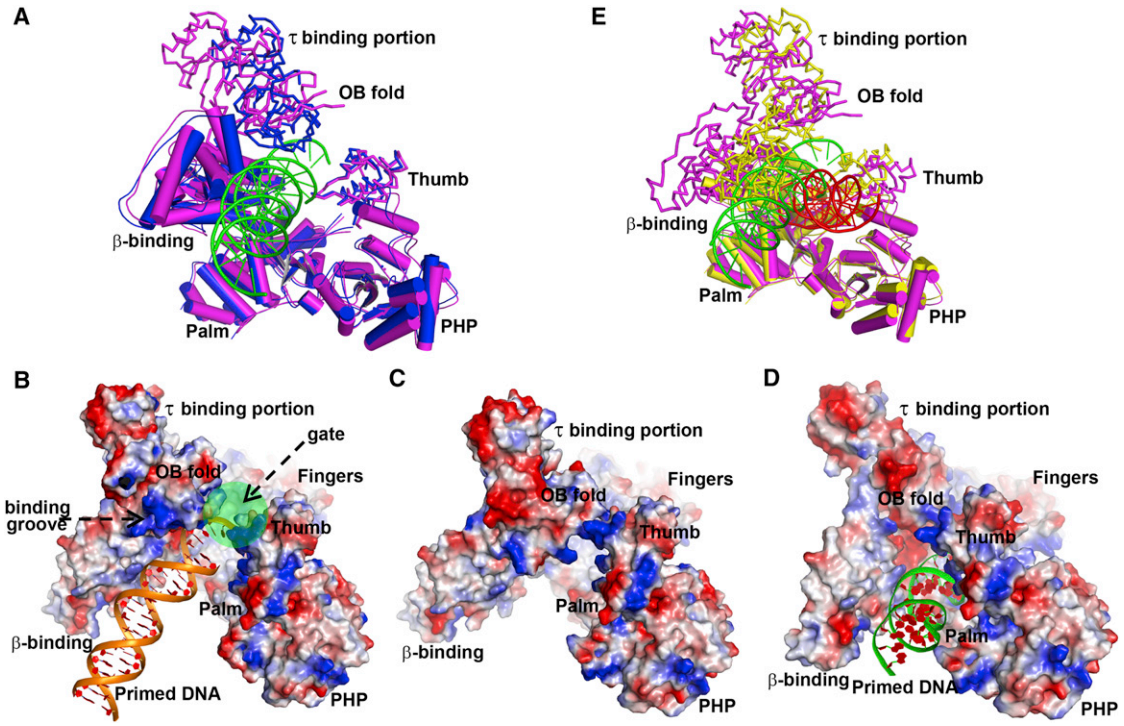

Figure 3. Comparison among the PolIIIα-τ_c-DNA Complex (Open Form), apo-PolIIIα, and PolIIIα-DNA Complex (Closed Form)

(A) Superimposition of the structure of the open form (magenta) and the apo structure (blue) on their PHP, palm, finger, and β-binding domains shows the differences in the positions of the CTD and the thumb domain.

(B–D) Electrostatic surface representations of the polymerase molecules in these forms are displayed by PyMOL.

(B) The gate (labeled with a green circle) of the PolIIIα-τ_c-DNA complex is open and the potential DNA binding groove faces away from the active-site cavity.

(C and D) The gates in the apo structure (C) and PolIIIα-DNA complex (D) are closed.

(E) The significant structural differences between the open form (magenta) and the closed form (yellow) are seen in the orientations of the CTD, thumb domain, β-binding domain, and DNA by superimposing their PHP, palm, and finger domains. The DNA substrates in them are green and red, respectively.

of the predicted loop and C-terminal helix of the *Eco*τ_c could completely disrupt the PolIIIα-τ_c interaction, and that the mutations in the beginning part of the helix and the possible loop region had larger effects on the binding of PolIIIα (Jergic et al., 2007). Also, the region of *Eco*PolIIIα that may bind to *Eco*τ_c was identified in mutagenesis studies and appears to be located in its unstructured extreme C terminus (Dohrmann and McHenry, 2005), which appears to be an α helix in this complex. Therefore, all of these data suggest that the loop and the beginning part of the helix may be close to or contact the polymerase tail, and may play a more important role in stabilizing the τ_c-PolIIIα interface in the *E. coli* system. One region of *Taq*τ_c (residues 525–534) makes similar interactions in the four copies and constitutes 83.2% of all the PolIIIα-the CTD of τ_c interface areas. The average rmsd of their Cα atoms is 0.95 Å.

PolIIIα in Complex with τ_c and DNA Displays an Open Form

The conformation of PolIIIα in this complex is different from that of the apo enzyme, with the most notable differences being the orientations of the CTD and the thumb domain (Figure 3A; Bailey et al., 2006). The new orientation of the CTD results in part from a rigid-body movement of ~12 Å along the y axis of the plane of Figure 3, as well as a 15° rotation of the τ-binding portion and a 5° rotation of the OB fold along the x axis, which leads to the increased angle between the OB fold and the τ-binding portion. These movements position the ssDNA-binding groove on the OB fold facing away from the active-site cavity instead of toward the DNA-binding site on the thumb domain, as observed in the apo structure (Figures 3B and 3C). In addition, this displacement, together with the movement of the thumb domain (a rotation of 5° along the x axis), results in the formation of an open gate conformation that would enable the entrance or exit of the DNA substrate from the active-site cavity. The gate is closed in both the apo structure and the structure of the complex with only DNA bound (Figures 3C and 3D). Since τ_c makes extensive contacts with all three portions of the CTD (Figure 2), these conformational changes might result from the binding of τ_c; however, the influence of crystal packing may be a larger factor. Because the complex assumes a less compact structure, we call it the open form. Furthermore, superimposition of this open form on the previous structure of PolIIIα in complex with DNA, which we call the closed form (Figure 3E; Wing et al., 2008), shows that the binding of the DNA substrate to the complex of PolIIIα with τ_c will induce significant conformational changes to form the closed conformation of the complex that is used during the leading and lagging strand DNA replication (Evans et al., 2008; McHenry, 2011). The structure of the complex presented here is influenced by crystal packing; nevertheless, the structure of this complex shows the position of τ_c on the polymerase and

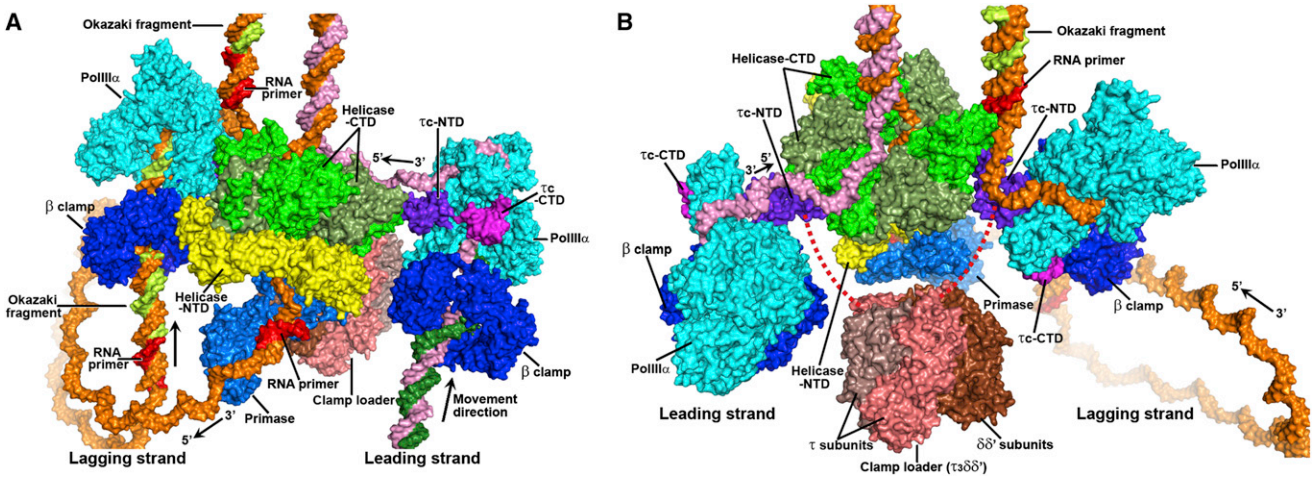

Figure 4. Atomic Model of the Replisome Structure at the Replication Fork

(A and B) The surface representations of these replisome components are displayed along two different directions. PolIIIα, β clamp, the NTD of τ_c, the CTD of τ_c, primase, and the NTD of helicase are labeled with cyan, blue, purple, magenta, marine, and yellow, respectively. The CTDs of helicase are labeled with green and dark green. The five subunits of the clamp loader are labeled with salmon, deep salmon, and brown. The red dashed lines represent the loop linking the two domains of the τ subunit. The modeled DNA strands are labeled with orange and pink for the mother strands, and with lime and forest for the daughter ones. The RNA primers are labeled with red.

See also Movie S1.

thus provides the first step in understanding how PolIIIα is positioned on DnaB helicase.

Atomic Model of the Replisome Structure at the Replication Fork

PolIIIα, β clamp, clamp loader, primase, τ_c, and helicase are important components of the replisome. The structure of the complex in this study, together with recent crystal structures of different replisome complexes, allowed us to construct a structural model of these components assembled at the replication fork (Figure 4). We chose the closed form of the polymerase (Wing et al., 2008) for the model of PolIIIα at the replication fork because it is the conformation of the enzyme during the DNA replication. We then mapped the structure of the *E. coli* β clamp in complex with DNA (Protein Data Bank [PDB] code: 3BEP; Georgescu et al., 2008a) onto the PolIIIα-DNA complex by superimposing their DNA substrates. The putative internal β-binding region (Dohrmann and McHenry, 2005) contacts the hydrophobic groove on the β clamp (Georgescu et al., 2008b) in the model perfectly. The length of DNA substrate from the active site in the palm domain to the β-clamp ring is ~24 bp (~80 Å). We subsequently positioned τ_c onto the PolIIIα-β-clamp DNA model by superimposing the CTDs of the two forms of PolIIIα. Because the CTD of the helicase ring (Haroniti et al., 2004; Martínez-Jiménez et al., 2002) has been shown to interact with the NTD of τ_c (Gao and McHenry, 2001a), the helicase ring was positioned in our model to contact the NTD of τ_c, as proposed in the previous atomic force microscopy model (Haroniti et al., 2004). The structure of the DnaB helicase in complex with ssDNA was utilized here (Itsathitphaisarn et al., 2012). It appears that the proposed interaction of helicase and τ in this model could also accommodate the observed τ-β-binding domain contacts in the structure of the complex. However, since high-resolution structural data on the interactions between the helicase and τ_c have not yet been obtained, the orientations and conformations of the helicase ring and τ_c are currently only a guess. The primase (PDB code: 2AU3; Corn et al., 2005) and the clamp-loader complex (PDB code: 3GLH; Simonetta et al., 2009) were docked into the model according to previously proposed models (Bailey et al., 2007; Haroniti et al., 2004). In addition, the model presented here contains only two polymerases, but recent studies have shown that a third polymerase may be involved during DNA replication (Georgescu et al., 2012; Reyes-Lamothe et al., 2010).

EXPERIMENTAL PROCEDURES

Cloning, Expression, and Purification

See Supplemental Experimental Procedures for details regarding vector construction. *T. aquaticus* PolIIIα was expressed and purified as described previously (Bailey et al., 2006). Purification of the τ_c fragment was achieved by heat treatment and Co^{2+} affinity chromatography (see Supplemental Experimental Procedures for further details).

Formation of the PolIIIα-τ_c-DNA Complex

The purified PolIIIα was mixed with an excess of τ_c and purified through gel filtration chromatography (see Supplemental Experimental Procedures for details). The PolIIIα-τ_c-DNA complex was formed by directly mixing the PolIIIα-τ_c complex with 10 mM $MgCl_2$, ddCTP (1 mM), dATP (1 mM), and a 2-fold molar excess of the preformed DNA substrate (primer sequence: 5′-cgaaacgacggccagtgcca-3′; template sequence: 5′-ttttttgtggcactggccgtc gtttcg-3′) at room temperature.

Crystallization, Data Collection, and Processing

Crystals of the ternary complex were grown for 2–3 days after setting up the drop with a 1:1 ratio of the complex sample to the initial well solution (0.1 M TRIS pH 8.8, 18% [w/v] polyethylene glycol 4000, 0.2 M $MgCl_2$) by using the sitting drop vapor diffusion method at 12°C. Crystal diffraction was improved to ~3–3.5 Å by optimizing conditions and utilizing a dehydration procedure (see Supplemental Experimental Procedures for further details). Derivatives were prepared by directly soaking dehydrated crystals in the drops containing

10 mM K_2PtCl_4 or 10 mM $HgCl_2$ for 30 min. Data sets were collected at 100 K using beamline 8.2.2 at the Advanced Light Source of (ALS) Lawrence Berkeley National Laboratory and beamline X-25 at the National Synchrotron Light Source (NSLS) of Brookhaven National Laboratory. All data were integrated and scaled using both the HKL2000 suite of programs (Otwinowski and Minor, 1997) and IMOSFLM (Leslie, 1999) plus SCALA (Bailey, 1994). The H test in the processing showed that the data sets were pseudomerohedrally twinned with a twinning operator (-h, -k, l).

Structure Determination and Refinement

The twinned data were used to solve the structure. Initially, individual domains of the apo *Taq*PolIIIα (PDB code: 2HPI) were utilized as the searching models with PHASER (McCoy et al., 2007). However, only the PHP, palm, β-binding, and finger domains could be located using native data sets, which may be due to the presence of pseudomerohedral twinning with an operator (-h, -k, l). Therefore, the SAD phases were then combined with the partial phases obtained by MR using PHENIX programs (Adams et al., 2010). Difference Fourier maps calculated using the combined phases located 24 platinum atoms or eight mercury atoms. The platinum atoms are bound to the surface methionine residues on the PHP, palm, finger, and β-binding domains (Figure S1A), whereas the mercury atoms are observed to bind to the cysteine on the CTD of PolIIIα and one tryptophan on the τ_c (Figure S1B). The thumb domains were clearly placed using combined phase with platinum derivative using COOT (Emsley and Cowtan, 2004). The combined phase with mercury derivative gave better density maps for the CTD and τ_c. Phases were improved through density modification, including multidomain averaging using NCSMASK (Bailey, 1994) and DM (Cowtan, 1999; Figures S1C and S1D). Cross-averaging among different crystals could not be performed in this study because the twinning fractions of different crystals vary. The model was then transferred to the higher-resolution native data set through MR using PHASER. Further multidomain averaging was also performed and the whole PolIIIα was then rebuilt using COOT. The τ_c model was initially built using the combined phases and then improved using the native data set to continue refinement, side-chain assignment, and residue location (Figure S2). The final electron density map allowed us to build the N-terminal and C-terminal portions of τ_c, but the linker loop was disordered. After the whole PolIIIα was rebuilt, the F_o-F_c difference maps clearly showed the density for the DNA substrates (Figure S3). Initial rigid-body refinements were performed by assigning 40 rigid domains and including the amplitude-based twin refinement using REFMAC 5 (Murshudov et al., 1997) with the twinned data. Further restrained refinements were performed by including translation, liberation, screw-rotation displacement refinement; twin refinement; and noncrystallographic symmetry restraints with the twinned data. Structure validation was performed using PROCHECK (Laskowski et al., 1993). The data collection and refinement statistics are shown in Table 1. All figures were created using PyMOL (DeLano, 2002). The interfaces of the complex were analyzed using AREAIMOL (Lee and Richards, 1971) and the PISA service at the European Bioinformatics Institute (http://www.ebi.ac.uk/pdbe/prot_int/pistart.html; Krissinel and Henrick, 2007).

SUPPLEMENTAL INFORMATION

Supplemental Information includes Supplemental Experimental Procedures, six figures, and one movie and can be found with this article online at http://dx.doi.org/10.1016/j.str.2013.02.002.

ACKNOWLEDGMENTS

We thank the staff at ALS beamline 8.2.2 and NSLS beamline X-25. We also thank R.C. Wilmouth and L.S. Lai for helpful discussions and the staff of the CSB core at Yale. B.L. performed experiments and solved the structure. J.Z.L. provided assistance in phase determination. B.L. and T.A.S. wrote the manuscript. This work was supported by both HHMI funding and NIH grant GM57510 to T.A.S.

Received: December 4, 2012
Revised: January 22, 2013
Accepted: February 1, 2013
Published: March 7, 2013

REFERENCES

Adams, P.D., Afonine, P.V., Bunkóczi, G., Chen, V.B., Davis, I.W., Echols, N., Headd, J.J., Hung, L.W., Kapral, G.J., Grosse-Kunstleve, R.W., et al. (2010). PHENIX: a comprehensive Python-based system for macromolecular structure solution. Acta Crystallogr. D Biol. Crystallogr. *66*, 213–221.

Bailey, S.; Collaborative Computational Project, Number 4. (1994). The CCP4 suite: programs for protein crystallography. Acta Crystallogr. D Biol. Crystallogr. *50*, 760–763.

Bailey, S., Wing, R.A., and Steitz, T.A. (2006). The structure of *T. aquaticus* DNA polymerase III is distinct from eukaryotic replicative DNA polymerases. Cell *126*, 893–904.

Bailey, S., Eliason, W.K., and Steitz, T.A. (2007). Structure of hexameric DnaB helicase and its complex with a domain of DnaG primase. Science *318*, 459–463.

Brautigam, C.A., and Steitz, T.A. (1998). Structural and functional insights provided by crystal structures of DNA polymerases and their substrate complexes. Curr. Opin. Struct. Biol. *8*, 54–63.

Corn, J.E., Pease, P.J., Hura, G.L., and Berger, J.M. (2005). Crosstalk between primase subunits can act to regulate primer synthesis in trans. Mol. Cell *20*, 391–401.

Cowtan, K. (1999). Error estimation and bias correction in phase-improvement calculations. Acta Crystallogr. D Biol. Crystallogr. *55*, 1555–1567.

DeLano, W.L. (2002). The PyMOL Molecular Graphics System (San Carlos, CA: DeLano Scientific).

Dohrmann, P.R., and McHenry, C.S. (2005). A bipartite polymerase-processivity factor interaction: only the internal beta binding site of the alpha subunit is required for processive replication by the DNA polymerase III holoenzyme. J. Mol. Biol. *350*, 228–239.

Emsley, P., and Cowtan, K. (2004). Coot: model-building tools for molecular graphics. Acta Crystallogr. D Biol. Crystallogr. *60*, 2126–2132.

Evans, R.J., Davies, D.R., Bullard, J.M., Christensen, J., Green, L.S., Guiles, J.W., Pata, J.D., Ribble, W.K., Janjic, N., and Jarvis, T.C. (2008). Structure of PolC reveals unique DNA binding and fidelity determinants. Proc. Natl. Acad. Sci. USA *105*, 20695–20700.

Gao, D., and McHenry, C.S. (2001a). tau binds and organizes *Escherichia coli* replication proteins through distinct domains. Domain IV, located within the unique C terminus of tau, binds the replication fork, helicase, DnaB. J. Biol. Chem. *276*, 4441–4446.

Gao, D., and McHenry, C.S. (2001b). tau binds and organizes *Escherichia coli* replication through distinct domains. Partial proteolysis of terminally tagged tau to determine candidate domains and to assign domain V as the alpha binding domain. J. Biol. Chem. *276*, 4433–4440.

Georgescu, R.E., Kim, S.S., Yurieva, O., Kuriyan, J., Kong, X.P., and O'Donnell, M. (2008a). Structure of a sliding clamp on DNA. Cell *132*, 43–54.

Georgescu, R.E., Yurieva, O., Kim, S.S., Kuriyan, J., Kong, X.P., and O'Donnell, M. (2008b). Structure of a small-molecule inhibitor of a DNA polymerase sliding clamp. Proc. Natl. Acad. Sci. USA *105*, 11116–11121.

Georgescu, R.E., Kurth, I., and O'Donnell, M.E. (2012). Single-molecule studies reveal the function of a third polymerase in the replisome. Nat. Struct. Mol. Biol. *19*, 113–116.

Haroniti, A., Anderson, C., Doddridge, Z., Gardiner, L., Roberts, C.J., Allen, S., and Soultanas, P. (2004). The clamp-loader-helicase interaction in Bacillus. Atomic force microscopy reveals the structural organisation of the DnaB-tau complex in Bacillus. J. Mol. Biol. *336*, 381–393.

Itsathitphaisarn, O., Wing, R.A., Eliason, W.K., Wang, J.M., and Steitz, T.A. (2012). The hexameric helicase DnaB adopts a nonplanar conformation during translocation. Cell *151*, 267–277.

Jergic, S., Ozawa, K., Williams, N.K., Su, X.C., Scott, D.D., Hamdan, S.M., Crowther, J.A., Otting, G., and Dixon, N.E. (2007). The unstructured C-terminus of the tau subunit of *Escherichia coli* DNA polymerase III holoenzyme is the site of interaction with the alpha subunit. Nucleic Acids Res. *35*, 2813–2824.

Johnson, A., and O'Donnell, M. (2005). Cellular DNA replicases: components and dynamics at the replication fork. Annu. Rev. Biochem. *74*, 283–315.

Kim, S., Dallmann, H.G., McHenry, C.S., and Marians, K.J. (1996). Coupling of a replicative polymerase and helicase: a tau-DnaB interaction mediates rapid replication fork movement. Cell *84*, 643–650.

Kong, X.P., Onrust, R., O'Donnell, M., and Kuriyan, J. (1992). Three-dimensional structure of the beta subunit of *E. coli* DNA polymerase III holoenzyme: a sliding DNA clamp. Cell *69*, 425–437.

Krissinel, E., and Henrick, K. (2007). Inference of macromolecular assemblies from crystalline state. J. Mol. Biol. *372*, 774–797.

Lamers, M.H., Georgescu, R.E., Lee, S.G., O'Donnell, M., and Kuriyan, J. (2006). Crystal structure of the catalytic alpha subunit of *E. coli* replicative DNA polymerase III. Cell *126*, 881–892.

Laskowski, R.A., MacArthur, M.W., Moss, D.S., and Thornton, J.M. (1993). PROCHECK: A program to check the stereochemical quality of protein structures. J. Appl. Cryst. *26*, 283–291.

Lee, B., and Richards, F.M. (1971). The interpretation of protein structures: estimation of static accessibility. J. Mol. Biol. *55*, 379–400.

Leslie, A.G.W. (1999). Integration of macromolecular diffraction data. Acta Crystallogr. D Biol. Crystallogr. *55*, 1696–1702.

López de Saro, F.J., Georgescu, R.E., and O'Donnell, M. (2003). A peptide switch regulates DNA polymerase processivity. Proc. Natl. Acad. Sci. USA *100*, 14689–14694.

Maki, H., and Kornberg, A. (1985). The polymerase subunit of DNA polymerase III of *Escherichia coli*. II. Purification of the alpha subunit, devoid of nuclease activities. J. Biol. Chem. *260*, 12987–12992.

Martínez-Jiménez, M.I., Mesa, P., and Alonso, J.C. (2002). *Bacillus subtilis* τ subunit of DNA polymerase III interacts with bacteriophage SPP1 replicative DNA helicase G40P. Nucleic Acids Res. *30*, 5056–5064.

McCoy, A.J., Grosse-Kunstleve, R.W., Adams, P.D., Winn, M.D., Storoni, L.C., and Read, R.J. (2007). Phaser crystallographic software. J. Appl. Cryst. *40*, 658–674.

McHenry, C.S. (1988). DNA polymerase III holoenzyme of *Escherichia coli*. Annu. Rev. Biochem. *57*, 519–550.

McHenry, C.S. (2011). DNA replicases from a bacterial perspective. Annu. Rev. Biochem. *80*, 403–436.

Murshudov, G.N., Vagin, A.A., and Dodson, E.J. (1997). Refinement of macromolecular structures by the maximum-likelihood method. Acta Crystallogr. D Biol. Crystallogr. *53*, 240–255.

Otwinowski, Z., and Minor, W. (1997). Processing of X-ray diffraction data collected in oscillation mode. In Methods in Enzymology, C.W. Carter and R.M. Sweet, eds. (New York: Academic Press), pp. 307–326.

Pritchard, A.E., Dallmann, H.G., Glover, B.P., and McHenry, C.S. (2000). A novel assembly mechanism for the DNA polymerase III holoenzyme DnaX complex: association of deltadelta' with DnaX(4) forms DnaX(3)deltadelta'. EMBO J. *19*, 6536–6545.

Reyes-Lamothe, R., Sherratt, D.J., and Leake, M.C. (2010). Stoichiometry and architecture of active DNA replication machinery in *Escherichia coli*. Science *328*, 498–501.

Romier, C., Dominguez, R., Lahm, A., Dahl, O., and Suck, D. (1998). Recognition of single-stranded DNA by nuclease P1: high resolution crystal structures of complexes with substrate analogs. Proteins *32*, 414–424.

Scheuermann, R.H., and Echols, H. (1984). A separate editing exonuclease for DNA replication: the epsilon subunit of *Escherichia coli* DNA polymerase III holoenzyme. Proc. Natl. Acad. Sci. USA *81*, 7747–7751.

Simonetta, K.R., Kazmirski, S.L., Goedken, E.R., Cantor, A.J., Kelch, B.A., McNally, R., Seyedin, S.N., Makino, D.L., O'Donnell, M., and Kuriyan, J. (2009). The mechanism of ATP-dependent primer-template recognition by a clamp loader complex. Cell *137*, 659–671.

Stano, N.M., Chen, J., and McHenry, C.S. (2006). A coproofreading $Zn^{(2+)}$-dependent exonuclease within a bacterial replicase. Nat. Struct. Mol. Biol. *13*, 458–459.

Steitz, T.A. (1999). DNA polymerases: structural diversity and common mechanisms. J. Biol. Chem. *274*, 17395–17398.

Studwell-Vaughan, P.S., and O'Donnell, M. (1991). Constitution of the twin polymerase of DNA polymerase III holoenzyme. J. Biol. Chem. *266*, 19833–19841.

Su, X.C., Jergic, S., Keniry, M.A., Dixon, N.E., and Otting, G. (2007). Solution structure of Domains IVa and V of the tau subunit of *Escherichia coli* DNA polymerase III and interaction with the alpha subunit. Nucleic Acids Res. *35*, 2825–2832.

Taft-Benz, S.A., and Schaaper, R.M. (2004). The theta subunit of *Escherichia coli* DNA polymerase III: a role in stabilizing the epsilon proofreading subunit. J. Bacteriol. *186*, 2774–2780.

Wing, R.A., Bailey, S., and Steitz, T.A. (2008). Insights into the replisome from the structure of a ternary complex of the DNA polymerase III alpha-subunit. J. Mol. Biol. *382*, 859–869.

Yao, N.Y., and O'Donnell, M. (2009). Replisome structure and conformational dynamics underlie fork progression past obstacles. Curr. Opin. Cell Biol. *21*, 336–343.

Yao, N.Y., and O'Donnell, M. (2010). SnapShot: the replisome. Cell *141*, 1088, 1088.e1.

